

A. van Blaaderen

Quantitative real-space analysis of colloidal structures and dynamics with confocal scanning light microscopy

Dr. A. van Blaaderen (✉)
Van't Hoff Laboratory
Debye Research Institute
Utrecht University
Postbus 80051
3508 TB Utrecht, The Netherlands

A. van Blaaderen
FOM Institute for Atomic
and Molecular Physics
Postbus 41883
1009 DB Amsterdam, The Netherlands

Abstract Quantitative real-space coordinates of 3D structures can be obtained with confocal microscopy on concentrated dispersions of index-matched silica spheres with a fluorescent particle core. The possibilities and limitations of this technique to probe 3D colloidal particle structures (e.g., glasses, crystals, gels and electro-rheological fluids) and dynamics of colloidal processes (e.g.,

diffusion, glass formation and phase separation) are discussed based on examples from the literature and new preliminary work presented in this paper. Extension of the method to the study of multi-component dispersions (e.g., binary crystals and glasses) is addressed as well.

Key words Confocal microscopy – silica – colloids – real-space

Introduction

Almost a century ago Perrin studied individual colloidal particles in real space to determine Avogadro's number [1]. After this pioneering work structural and dynamic information on colloidal particle systems was mainly obtained with scattering techniques [2]. Recently, quantitative real-space techniques have become more feasible through technical advances in both data acquisition and data processing [3–6]. Usually, the approach is to image individual particles and to extract information by image analysis. However, it is possible to obtain quantitative information without visualizing colloids separately [7, 8]. Individual particles are mostly imaged in two-dimensional (2D) systems with digital video microscopy. Examples include work on phase transitions [9–11], diffusion [12, 13] and the measurement of pair potentials [14–16]. The first few layers of particles close to the container wall of three-dimensional (3D) crystals [17, 18] and crystallization [19] have also been studied. The cause for this limitation to image only close to the glass wall is twofold. First, the imaging of unmatched relatively large colloids is

hindered by significant scattering and loss of intensity deeper inside even not too concentrated dispersions. Second, with conventional microscopy, out-of-focus light contributes to the image and makes it hard to distinguish colloids deep in the bulk of concentrated dispersions even if the index is matched. There are several solutions to these problems. For instance, by only imaging tracer core-shell particles in an otherwise matched concentrated dispersion it is possible to measure diffusion of the tracer particles in a 2D plane inside the bulk [20]. Also, interactions between two particles can be measured away from the glass walls in a dilute dispersion after placing them in the focal plane with optical tweezers [15]. The solution reviewed in this paper is confocal scanning laser microscopy (CSLM) on matched dispersions of fluorescent core-shell silica spheres and the aim of the paper is to discuss the strong and weak points of this real-space technique through a number of examples taken from published, earlier work and preliminary, new results.

In confocal fluorescence microscopy the field of view is limited to a diffraction limited spot. This spot excites a fluorescent dye and the fluorescent light is imaged by the

same (confocal) high numerical aperture lens onto a point detector. Light that lies outside the focal plane is imaged in front of or behind the detector pinhole and is strongly rejected. The result is the ability to take optical sections out of a 3D sample with a thickness of about 500 nm. In addition, the multiplication of the response of both a point source and point detector also leads to a higher resolution, about 250 nm in the plane of the optical section, compared to conventional light microscopy [4]. Confocal microscopy is already a well established technique for imaging biological structures and processes and also its use in characterization of integrated circuits is well documented [4]. 3D real-space imaging of colloidal particle structures in the bulk is relatively new [5]. In the first-papers the interpretation was difficult because individual particles could not be recognized [21] and/or because the colloids were not optically matched [23]. Particles with a fluorescent core and a refractive index close to that of the solvent made it possible to distinguish individual spheres even in concentrated dispersions [23] and to obtain semi-quantitative results on colloidal crystal growth rates [24] and the stacking order of close packed planes of colloidal crystals in the bulk of a dispersion [25]. The stacking order of hard-sphere crystals has also been obtained recently using phase contrast microscopy on index-matched dispersions [26]. As explained in Ref. [3] optical sectioning is possible with differential interference contrast as well. However, until now, quantitative particle positions in the bulk of 3D structures have only been obtained with confocal microscopy after a measurement of the convolution of the point spread function of the confocal microscope with the fluorescent sphere and subsequent digital image analysis [27].

In the following, the possibilities and limitations of the real-space technique to obtain quantitative data on *stationary structures, dynamics* and *multi-component dispersions* will be discussed after a brief experimental section.

Experimental

Particle synthesis and characterization are described in the literature [24, 28]. The preliminary experiments described here were performed with fluoresceine labeled spheres with a final radius of 525 nm (fluorescent core 200 nm, relative standard deviation in size, $\sigma = 2\%$) and two kinds of rhodamine labeled spheres with the same fluorescent core (radius 100 nm) and a final radius of 210 nm ($\sigma = 6\%$) and 460 nm ($\sigma = 2\%$).

More extensive experimental details of the preliminary experiments presented in this paper will be given elsewhere. The gel was made from an initial volume fraction of

fluoresceine labeled spheres in a matching mixture of glycerol and water containing 4 wt % tetramethylammonium hydroxide. The gellation was initiated by addition of methylformate which slowly hydrolyzed to methanol and formic acid causing the particles to aggregate. Because of the relatively slow initial change in pH there is time to fill a capillary before aggregation commences. The electro-rheological fluid consisted of the fluoresceine labeled spheres dispersed in a matching mixture of glycerol and water. The applied alternating field strength was $1 \text{ V}/\mu\text{m}$ with a frequency of 3 MHz which is much faster than the relaxation time in the double layer. The electrodes were formed by indium-tin-oxide (ITO) coated glass cover slides. The charged glass-and-crystalline sample was quenched from an initial volume fraction of 40% of the fluoresceine labeled spheres in dimethylformamide (DMF) with 0.001 M LiCl. Also the two binary mixtures were made in DMF (0.01 M LiCl) with the mixture of the spheres with almost the same size consisting of a molar ratio of 100:1, fluoresceine labeled spheres to the rhodamine spheres (total radius 460 nm), volume fraction 55%. The mixture with the larger size ratio of 0.4 consisted of 50% volume fraction of fluoresceine labeled spheres and 20% volume fraction of the smaller rhodamine labeled spheres (total radius 210 nm).

The fluorescence confocal micrographs were made on two confocal set-ups: a Multiprobe 2001 of Molecular dynamics using a 100×1.4 numerical aperture lens on an inverted Nikon Diaphot microscope and a Leica TCS 4D confocal system with a 100×1.4 numerical aperture lens on a Leitz DM IRB inverted microscope.

The experimental method to find the particle positions will be described in more detail elsewhere [29], but, briefly, consists first of a measurement of the microscope response function of a single sphere. This is done by taking a 2D arrangement of spheres in immersion oil on a coverslip and measuring the intensity of each sphere in successive optical sections that are 100 nm apart. In each image plane the sphere positions and intensities are found in a similar way as has been described by Crocker and Grier [6]. By averaging over several hundred spheres the intensity distribution as a function of the z -coordinate (that is the coordinate along the optical axis of the microscope and perpendicular to the optical section plane or, xy -plane) was obtained accurately. Subsequently, the process is repeated on a series of optical sections, typically 100 sections 100 nm apart. In each plane particles are identified and the intensity determined. Out of all the xy -coordinates and intensities the approximate z -coordinate of the centers is determined by looking for maxima. Subsequently, only those intensities with approximately the same xy -coordinate in the different planes are taken together as belonging to one individual sphere. The final xy -coordinate is

determined by an intensity weighed average over the xy -positions from the different sections. To obtain accurate z -positions fits are performed using the measured functions for single spheres. If other spheres are too close above or below the sphere so that the intensities are overlapping this is taken into account.

Results and discussion

Stationary structures

3D coordinates of colloidal particles can clearly be obtained with the highest accuracy if the particles do not change their position during the time it takes to obtain a data set. Faster scan rates and consequently smaller dwell times per 3D volume element or voxel can be realized if the fluorescence intensity is increased by increasing the exciting light intensity, the amount of dye or the quantum yield of the dye used. There are several reasons however, why it is not desirable to increase the intensity of the scanning laser beam above certain levels. All organic dyes bleach and lose the ability to fluoresce after absorbing a certain amount of photons, dissipation of some of the absorbed light can cause heating and too many photons can saturate the fluorescense by overpopulating the excited state. Similarly, the concentration of the fluorophore is limited. Too high concentrations cause a decrease in fluorescent intensity by the creation of non radiative decay pathways and can also make the absorption so high it becomes difficult to probe the sample at any significant depth. Because of all these reasons, there is a lower limit to the dwell time per voxel. Roughly, this translates to about 0.25 s for a frame of 512×512 voxels and for the particles and dyes used in this study, fluoresceine and rhodamine, which have an optimized amount of dye per particle and further have a quantum yield that is close to the highest values reported for organic dyes [30]. As the determination of the z -coordinates requires several frames at different z -positions, the structure needs to be stationary for at least several seconds to obtain the coordinates without a blurring caused by motions.

There are several interesting colloidal particle structures which (almost) meet this requirement not to change on a time scale of seconds. The 3D real-space structure of glasses formed from particles interacting with a hard-sphere like potential is described in Ref. [27]. From a volume fraction of 60% until 64% there was no detectable particle movement and 10.000 sphere positions could be obtained in one measurement with high accuracy (about 15 nm in the plane of the optical section and 25 nm perpendicular to this plane). These measurements made it possible for the first time to test theories about the local

structure of a hard-sphere glass quenched from a colloidal liquid in thermodynamic equilibrium on experimental real-space data.

One other example is formed by colloidal crystals made again from particles interacting with a hard-sphere like potential. These crystals were grown through a directed growth on a template in a gravitational field, a new method called colloidal epitaxy [31]. Here the almost immobility of the particles away from their lattice positions was a consequence of the almost close packed volume fraction (around 74%) which was caused by the pressure of the layers of colloid compressing the crystal in the gravitational field. Further, not only the particle positions could be obtained accurately, but also the positions of the spheres in the crystal in relation to the holes in the polymer template could be determined by confocal microscopy. This was achieved by also incorporating into the polymer template a fluorescent dye, so that it could be imaged simultaneously with the sphere centers. It is also shown in this work that by mismatching the lattice constant of the template the resulting defect structures can be studied in detail in real-space. With scattering methods the study of such local irregularities as defects in crystals is very hard.

Gels and flocs can have sufficiently immobile particles as well. In Fig. 1a the 3D structure of a gel that resulted from reaction limited aggregation is shown. The scale of the figure is such that it is just possible to see the individual particles that make up the gel. If viewed with green (right eye) and red (right eye) glasses the depth than can be seen in this figure is striking. The voxel size shown in Fig. 1a is not small enough to obtain particle positions as shown in Fig. 1b, but the 3D image on this large scale gives an insight into the gel structure that is very hard to extract from scattering data, or from an extracted parameter like a fractal dimension. For instance, it can be seen in a direct way that the volume filling gel structure is build up out of more compact particle clumps. These more compact aggregates are a result of the rearrangements early on in the aggregation process as not every collision resulted in aggregation of the spheres. Subsequently, these relatively dense sub units cluster-cluster aggregated, while also sedimenting. By necessity the number of particles of which the coordinates was determined in Fig. 1b is much smaller and the average structure as given by the radial distribution function (not shown here) is not very accurate. Although it is experimentally possible to 'patch' together several connecting data sets as shown in Fig. 1b, this is a very lengthy and difficult process. Therefore, it is difficult to probe a 3D real-space structure over several decades to test for instance for the presence of a fractal dimension. Further, these kind of structures contain inhomogeneities over different length scales making it also harder to obtain a good average of the structure. However, even without

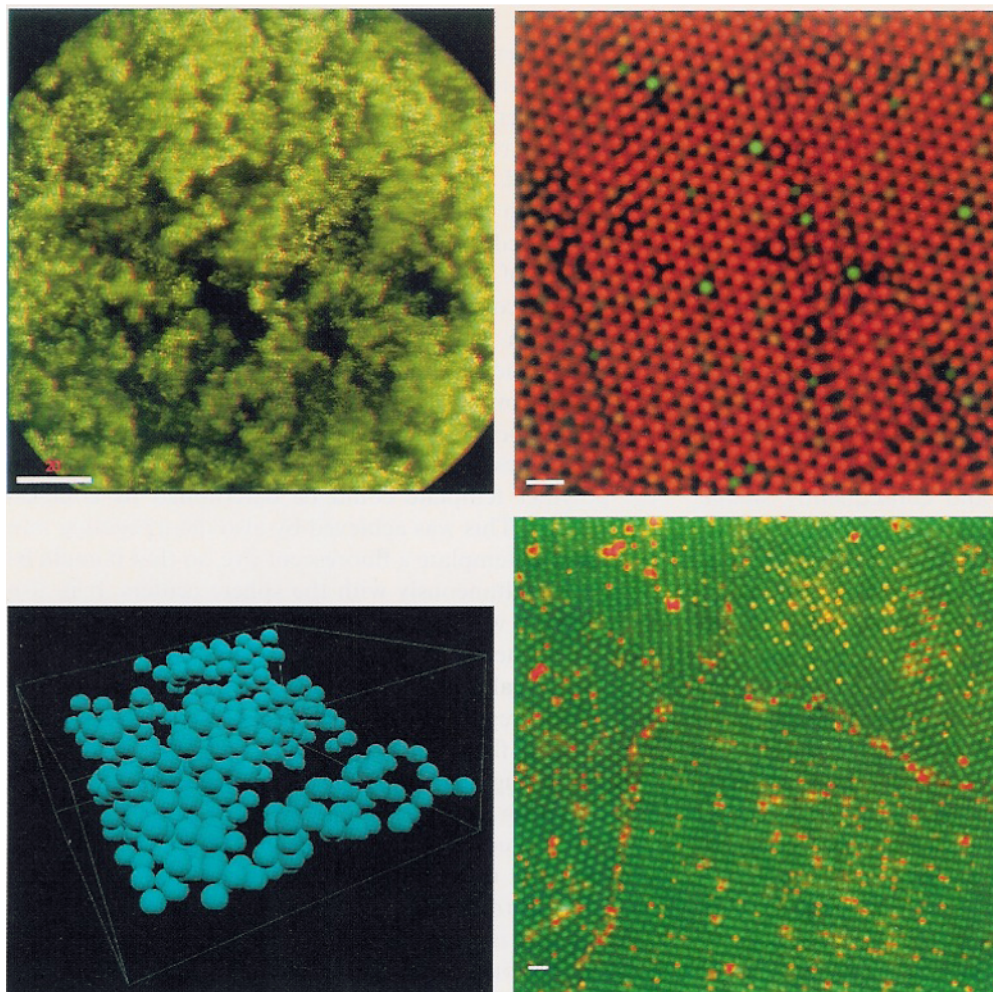


Fig. 1 Colloidal gel formed through reaction-limited aggregation of fluorescent-core (radius 200 nm) silica-shell particles (total radius 525 nm); volume fraction 20% in index-matched mixture of glycerol/water. Bar is 20 μm . (a) 3D confocal micrograph of the gel. (b) Computer generated picture of part of the gel after the particle coordinates were obtained from a 3D experimental data set (33 $\mu\text{m} \times 33 \mu\text{m} \times 9 \mu\text{m}$)

Fig. 4 Confocal micrographs of binary mixtures of fluorescein (total radius 525 nm) and rhodamine labeled spheres dispersed in DMF with 0.01 M LiCl. (a) Rhodamine labeled spheres with total radius of 460 nm, molar ratio of rhodamine to fluorescein labeled spheres: 100:1, total volume fraction 55%. (b) Rhodamine labeled spheres with total radius of 210 nm, volume fraction of rhodamine labeled spheres 20% of fluorescein labeled spheres 50%. Bars are 2 μm

good statistical averages the real-space measurements can provide for insights in the structure that can for instance be used to interpret and model scattering data.

A final example is presented in Fig. 2 where a confocal micrograph taken halfway between two ITO electrodes conveys the structure of an electro-rheological fluid. The relatively high alternating electric field (1 V/ μm , 3 MHz) is perpendicular to the optical section and the “strings” of particles that are visible in this section are in reality just 2D slices of sheets of particles where the normal of the sheets is perpendicular to the electric field. The sheets itself are built up from true, straight strings of spheres that are

parallel to the field lines. The curvature of the sheets, which is not changing in time, is what appears as the worm-like “strings” in the section of Fig. 2. The field strength, 1 V/ μm , at which these sheets were formed was so high that the dipolar interaction energy between two spheres was many times kT . Immobilization, and therefore a relative easy structure determination is made possible in this example because of this strong restraining, external field. Therefore, these sheets are very likely non-equilibrium structures, because it is generally accepted that a tetragonal crystalline arrangement of strings of spheres packed close together is the equilibrium phase at high fields. It is

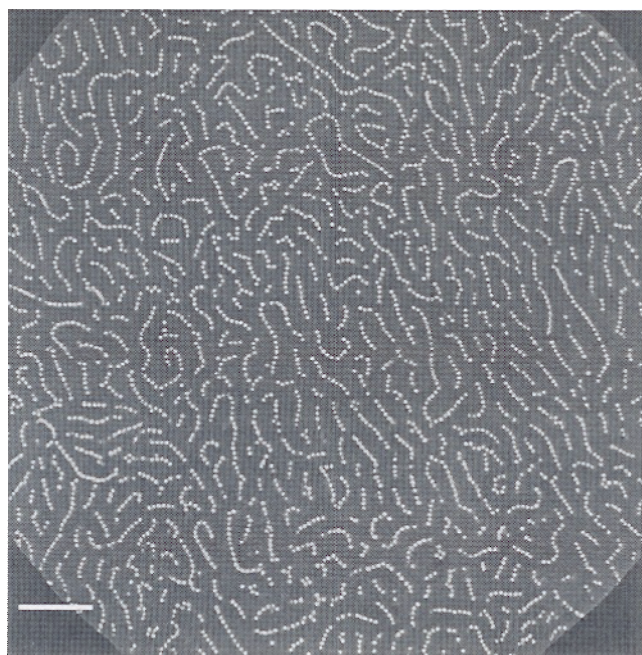


Fig. 2 Confocal micrograph of an electro-rheological fluid consisting of fluoresceine labeled spheres (total radius 512 nm) in a matching mixture of glycerol and water in between two ITO electrodes (10 μm apart). Field strength of 1 V/ μm (frequency 3 MHz) is perpendicular to the optical section which was taken halfway in between the electrodes. Bar is 20 μm

interesting to notice that exactly the same kind of sheets were observed in magneto-rheological fluids only if the magnetic field was increased to high values quickly so that no equilibrium phase could be reached [32]. Applications, like a variable transmission, will operate under high fields, because this will give the fastest and largest increase in viscosity. This one brief example demonstrates that a quantitative real-space analysis of the resulting (out of equilibrium) structures can be very revealing and helpful to find the most optimal conditions.

In the above-mentioned examples the structures were more or less stationary during a measurement. There is of course no reason to limit the structural measurements to these relatively rare occasions. For instance in the case of crystals made out of charged particles with extended double layers or hard-sphere crystals at volume fractions significantly below 74% the particles will diffuse around on the average lattice position and this will diminish the accuracy of the particle positions. The average structure or type of lattice can still be determined accurately.

Dynamics

It has been shown that by imaging a single particle in a small field of view coupled with fast image analysis and

a feedback mechanism the colloidal particle can be traced in 3D and its diffusion measured [33]. For a whole collection of particles in a concentrated dispersion this is much harder and has not yet been done. However, if the dynamics of the process, like gas-liquid like phase separation, or if the particle mobilities are isotropic, then in principle following x - y displacements in a thin optical section could give all necessary information. For tracer or (semi) 2D systems this has already been shown to give diffusion coefficients with an accuracy comparable to that of e.g., dynamic light scattering [20].

In Fig. 3a a section can be seen that was taken inside the bulk of a colloidal dispersion of charged particles (double layer thickness of 15 nm) that was quenched by centrifugation after crystallization had started. During twenty time steps of 5 s the particle positions in this 2D slice were followed as far as they did not go too far above or below the section. It can be seen that the crystalline regions did not grow, but also that in the glassy regions in between the crystals there still was substantial particle movement (Fig. 3b). From a movie made of the 20 sections it became obvious that these particle movements are not random but have a clear localized and “collective” component both in time and direction, unfortunately this cannot be seen in the figure. In other words, particles move together in more or less the same direction in a kind of bursts. Localized motions in “dynamic pockets” has also been observed by us in completely glassy, quenched dispersions of charged particles. If these first results are no artifacts and can be reproduced and quantified, this would be very important for an understanding of mobility in very condensed liquids or glasses. For instance, in mode coupling theory these very localized regions of particle mobility are not considered. The resemblance of Fig. 3 to a figure in Ref. [34] where also the dynamics in a 2D liquid has been described as kinetic structural inhomogeneous is striking.

Multi-component dispersions

With multiple labeling the real-space measurements can be extended to multi-component systems if multi-line excitation and multi-channel detection are possible on the confocal set-up. In Fig. 4a a binary crystal of fluoresceine labeled spheres (green, total radius 525 nm) and 13% smaller rhodamine labeled spheres (red, total radius 460 nm) can be seen. The minority fluoresceine labeled spheres form a solid-solution (although in this case “solid-gas” might be a better term) on the crystal lattice of smaller spheres. The crystal consists of a random stacking of hexagonal close-packed layers as is usually found for

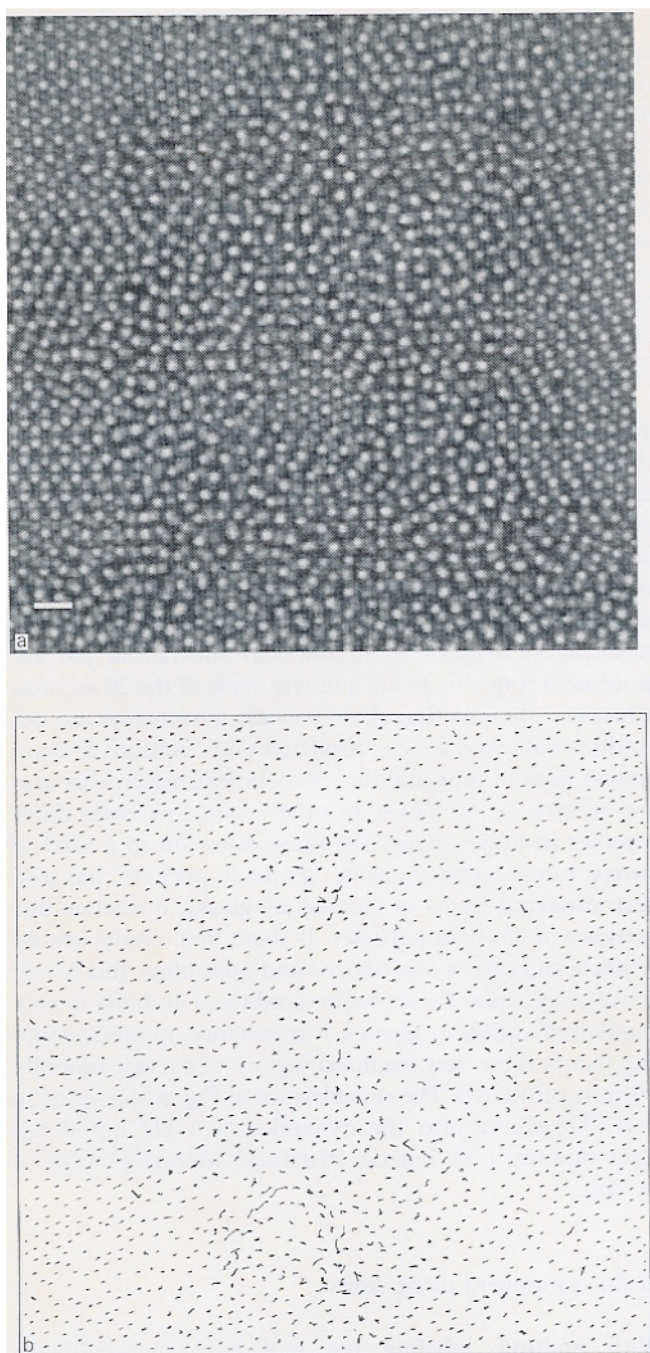


Fig. 3 Dynamics in the bulk of a crystalline/glassy charged colloidal system (DMF with 0.001 M LiCl). (a) Optical section at time = 0 s. (b) Particle trajectories of (most of) the particles present in (a) 20 time steps, 5 s apart. Bar 2 μm

hard-sphere like particles [31]. It will be very interesting to analyze the glasses that can be quenched from this binary system, because the size difference is such that, close to an optimal mixing ratio, icosahedral fragments can be formed

more easily than in a dispersion with just one size of spheres.

In the other example of a binary dispersion, Fig. 4b, one of the two components, the rhodamine labeled spheres (red, total radius 200 nm), cannot be resolved as separate spheres while the crystalline fluoresceine labeled spheres (green, total radius 525 nm) can be distinguished easily. There seems to be a preference of the small spheres for the grain boundaries and defects in the crystals of the larger spheres. Here and there the small spheres can be seen on lattice positions, but a definite AB or AB_2 crystalline structure has not (yet) been formed. In a fully developed binary crystalline structure, e.g., AB_2 , the average positions of the smaller spheres could still be determined. And even if this is not possible, like in the grain boundaries, the fluorescent intensity of the small spheres can be used to determine its local volume fraction. Similar measurements would be possible in a binary mixture consisting of (large) labeled spheres and labeled polymers.

Conclusions

The importance of real-space analysis of colloidal structures and dynamics is increasing, on the one hand because of the development of new and more quantitative methods, but also because the structures and processes under study are becoming more complex. Through examples it was shown that with confocal microscopy on matched dispersions of fluorescent-core silica-shell particles structures can be measured accurately inside bulk if the structure is stationary on a time scale of seconds. With a frame refresh rate of about 0.25 s (512^2 voxels) it is also possible to follow the dynamics of micron size particles in the bulk. If the motion of many particles needs to be followed, the analysis is at the moment limited to a (semi) 2D section of a section situated in the bulk. The examples shown in this paper have made it clear that although it is in some cases hard to get statistically good averages, the real-space information is of great use for a detailed description of complex structures and processes. The information can subsequently be used to model and interpret scattering data that generally give better averaged information. Finally, the extension of the method to multi-component systems that are labeled with fluorophores is straightforward and can even provide valuable information if one of the components cannot be resolved on the particle level.

Acknowledgments Pierre Wiltzius and Cherry Murray (Bell Laboratories, Lucent Technologies, where most of the measurements were done) are thanked for discussions and encouragement.

References

1. Perrin J (1910) *Brownian Motion and Molecular Reality*. Taylor and Francis, London
2. Pusey PN (1990) In: Levesque D, Hansen J-P, Zinn-Justin J (eds) *Liquids, Freezing and the Glass Transition*. Elsevier, Amsterdam
3. Inoué S (1986) *Video Microscopy*. Plenum, New York
4. Wilson T (ed) (1995) *Confocal Microscopy*. Academic Press, London
5. van Blaaderen A (1993) *Adv Mater* 5(1):52–55
6. Crocker JC, Grier DG (1996) *J Colloid Interface Sci* 179:298–310
7. Monovoukas Y, Gast AP (1991) *Langmuir* 7:460–468
8. Aastuen DJ, Clark NA, Cotter LK, Ackerson BJ (1986) *Phys Rev Lett* 57(14):1733–1736
9. Murray CA (1992) In: Strandburg KJ (ed) *Bond-Orientational Order in Condensed Matter Systems*, Ch. 4. Springer, New York
10. Helgesen G, Skjeltorp AT (1991) *Physica A* 170:488
11. Marcus AH, Rice SA (1996) *Phys Rev Lett* 77(12):2577–2580
12. Schaertl W, Sillescu H (1993) *J Colloid Interface Sci* 155:313
13. Marcus AH, Lin B, Rice SA (1996) *Phys Rev* 53:1765–1776
14. Kepler GM, Fraden S (1994) *Phys Rev Lett* 73:356–360
15. Crocker JC, Grier DG (1996) *Phys Rev Lett* 73:352–355
16. Vondermassen K, Bongers J, Mueller A, Versmold H (1994) *Langmuir* 10:1351
17. Hachisu S, Yoshimura S (1980) *Nature* 283:188–189
18. Grier DG, Murray CA (1994) *J Chem Phys* 100(12):9088–9095
19. Bongers J, Versmold H (1996) *J Chem Phys* 104(4):1519–1523
20. Kasper A, Kirsch S, Renth F, Bartsch E, Sillescu H (1996) *Progr Colloid Polym Sci* 100:151–155
21. Bremer LGB (1992) Thesis, University of Wageningen, Wageningen
22. Yoshida H, Ise N, Hashimoto T (1995) *J Chem Phys* 103:10146–10151
23. van Blaaderen A, Imhof A, Hage W, Vrij A (1992) *Langmuir* 8:1514–1517
24. Verhaegh NAM, van Blaaderen A (1994) *Langmuir* 10:1427–1438
25. Verhaegh NAM, van Duijneveldt JS, van Blaaderen A, Lekkerkerker HNW (1995) *J Chem Phys* 102:1416
26. Elliot MS, Bristol BTF, Poon WCK (1997) *Physica A* 235:216–223
27. van Blaaderen A, Wiltzius P (1995) *Science* 270:1177–1179
28. van Blaaderen A, Vrij A (1993) *Langmuir* 8:29221–2931
29. van Blaaderen A, Lubachevsky B, Wiltzius P, in preparation
30. Imhof A (1995) Thesis, Utrecht University, Utrecht
31. van Blaaderen A, Ruel R, Wiltzius P (1997) *Nature* 385:321–324
32. Lawrence EM, Ivey GA, Flores A, Liu J, Bibette J, Richard J (1994) *Int Mod Phys B* 8:2765–2777
33. Schätzel K, Neumann W-G, Müller J, Merzok B (1992) *Appl Opt* 31:770–778
34. Hurley MM, Harrowell P (1995) *Phys Rev E* 52:1694–1698